POLITECNICO DI TORINO
Repository ISTITUZIONALE

Evolution of CO2 Uptake Degree of Ordinary Portland Cement During Accelerated Aqueous
Mineralisation

(Article begins on next page)

05 February 2025

Article

Evolution of CO₂ Uptake Degree of Ordinary Portland Cement During Accelerated Aqueous Mineralisation

Giuseppe Ferrara [1,*] **, Pedro Humbert** [2] **, Davide Garufi** [2] **and Paola Palmero** [1]

1   INSTM R.U. PoliTO-LINCE, Department of Applied Science and Technology, Politecnico di Torino, Corso Duca Degli Abruzzi 24, 10129 Torino, Italy; paola.palmero@polito.it
2   Innovation Centre for Sustainable Construction, CRH, De Klencke 10, 1083 HL Amsterdam, The Netherlands; phumbert@crh.com (P.H.); dgarufi@crh.com (D.G.)
*   Correspondence: giuseppe.ferrara@polito.it

Abstract: The utilisation of carbonation treatments to produce building materials is emerging as a valuable strategy to reduce CO_2 emissions in the construction sector. It is of great importance to regulate the degree of carbonation when the mineralisation process is combined with hydration, as a high CO_2 uptake may impede the development of adequate strength. A significant number of studies focus on attaining the maximum carbonation degree, with minimal attention paid to the examination of the evolution of CO_2 uptake over the initial stages of the process. In this context, the present study aims to investigate the evolution of CO_2 uptake over time during carbonation. Ordinary Portland Cement (OPC) is employed as material, with aqueous carbonation selected as the mineralisation process. This investigation encompasses a range of carbonation durations, spanning from 5 to 40 min. The analysis of the evolution of the mineral composition with time demonstrated that the rate of the carbonation reaction accelerates in the initial minutes, resulting in the conversion of all the portlandite produced during the hydration process in the initial 10 min. Quantitative analysis of the carbonation degree indicated that the CO_2 uptake at 40 min is equal to 19.1%, which is estimated to be approximately 70% of the maximum achievable value. By contributing to the understanding of the early carbonation mechanisms in aqueous conditions of OPC, this study provides valuable support for further investigation focused on the use of cement mineralisation processes to produce building materials.

Keywords: cement; carbon capture and storage; accelerated carbonation; calcium carbonate; CO_2 uptake

1. Introduction

It is estimated that approximately 40% of the planet's energy resources are attributed to the construction sector [1]. Cement is responsible for approximately 7% of total greenhouse gas emissions due to its embodied energy and its extensive use, which is driven by the ever increasing global demand for concrete production [2]. In order to comply with the European Union's climate policy, it is imperative that urgent action be taken to achieve net zero emissions in the cement industry by 2050 [3].

The utilisation of natural raw products [4–7] or recycled materials [8] as a potential solution to reduce cement use is an emerging trend. Nevertheless, the complete replacement of cement remains impractical due to its mechanical properties and extensive availability. Recently, the utilisation of Carbon Capture and Utilisation (CCU) technologies has emerged as a potential strategy for significantly reducing CO_2 emissions in the building materials sector [2]. The reduction of CO_2 is achieved by inducing accelerated mineralisation of alkaline products, which results in permanent storage of CO_2 through the formation of stable calcium (or magnesium) carbonates. In addition to cement, a range of alkaline wastes and industrial byproducts can be employed in the carbonation processes, including steel slag, cement bypass dust and construction and demolition waste [9]. The mineralisation

process can be induced to produce either precast building blocks [10,11] or carbonated powder for use in a cement blend [12,13]. The aqueous carbonation method is a technique that is widely employed for the production of carbonated powder. The process entails the injection of CO_2 gas into an aqueous suspension comprising alkaline powder, with a liquid-to-solid ratio between 3 and 10. The process occurs by stirring the suspension until the carbonation is completed [14]. Subsequently, the slurry is subjected to centrifugation and drying, thereby obtaining the carbonated powder. Despite the promising results in terms of the carbonation degree, concerns have been raised regarding the mechanical performance of these powders when used as supplementary cementitious material [15,16]. An alternative approach involves carbonating fresh mixtures immediately prior to casting [17,18]. Cement powder, which is highly alkaline and rich in portlandite when hydrated, is an appropriate feedstock for aqueous carbonation. Monkman et al. (2017) proposed a methodology wherein CO_2 is injected during the mixing of fresh concrete, thereby facilitating the formation of nucleation sites for the development of hydrated calcium silicates [18]. This process results in enhanced mechanical strength of the concrete. Nevertheless, while elevated levels of CO_2 injection result in enhanced carbonation, exceeding a specific threshold can reverse this beneficial effect. An excess of calcium carbonate impedes the correct hydration process, which ultimately results in a reduction in the mechanical strength of the material [17]. These findings emphasise the importance of achieving a specific carbonation degree, which emerges as a crucial factor in defining the properties of the end product. This aspect is also emphasised by Matschei et al. (2007), who investigated the role of calcium carbonate in cement hydration. Their findings indicate that calcite in cement paste added as limestone acts both as an inert filler and an active participant in the hydration process [19]. In particular, it is assumed that all the calcite is reactive with cement up to a 5% content.

In case calcium carbonate is introduced in the form of limestone or pure $CaCO_3$, it is relatively straightforward to regulate its quantity within a given mixture. Conversely, when the presence of carbonates is derived from an accelerated carbonation process, it is challenging to obtain the desired amount, as it depends on the parameters of the mineralisation process. Specifically, once the water content of the mixture and the CO_2 flow have been fixed, it is of the utmost importance to determine the requisite time of injection in order to achieve the desired carbonation degree. Fu et al. (2024) proposed an innovative approach in which aqueous carbonated cement slurry is mixed with dry cement and aggregates to create concrete. They demonstrated that the duration of the mineralisation process affects the carbonation degree and, consequently, the mechanical properties of the end product, confirming the importance of controlling the carbonation degree [20].

The mechanisms of OPC-enforced carbonation have been extensively studied in the literature with respect to the kinetics of the clinker reaction and phase analysis of carbonation products [21]. Nevertheless, the investigation of the evolution of the CO_2 uptake evolution over time during OPC carbonation, evaluated through established testing procedures documented in the literature [22–24] and currently under investigation by an international scientific committee [25], remains a gap in the field. Indeed, the majority of studies examining the carbon capture of cement-based materials in aqueous conditions utilise pulverised hydrated cement paste, either created in a laboratory setting or derived from concrete demolition waste [26–30]. The use of raw cement powder is less prevalent.

In order to address this knowledge gap, the present study aims to investigate the evolution of the carbonation degree during the aqueous mineralisation of OPC powder, adopting a similar approach to that used for other cement-based materials. This implies the rigorous quantification of the stored CO_2, which is a pivotal element in the formulation of a comprehensive cost-benefit analysis with a view to achieving zero net CO_2 emissions in the cement value chain [31,32]. To this purpose, a number of different timescales for the carbonation process were considered. The objective of the investigation of mineral composition is twofold: firstly, to identify the compounds involved in the process and secondly, to qualitatively observe the development of calcium carbonate with mineralisation time. Furthermore, quantitative analysis, such as thermogravimetric and thermal

decomposition in a muffle furnace, was employed to provide quantitative information concerning carbonate content. The CO_2 uptake and carbonation efficiency were evaluated in accordance with established equations from the literature [22–25]. Ultimately, to provide a comprehensive analysis of the efficiency of cement powder aqueous carbonation, the results are compared with those of analogous studies that have employed cement-based materials in aqueous carbonation processes.

2. Materials and Methods

2.1. Cement Characterisation

The raw material selected for use was Ordinary Portland Cement (CEM I 52.5 N). The as-received powder was subjected to physical and chemical characterisation. The particle size distribution was assessed by means of laser granulometry (Malvern Mastersizer 3000E laser diffraction particle size analyser, Worcestershire, UK), and the results are presented in Figure 1, which shows the frequency and cumulative volume distribution. The percentile values, d90, d50, and d10, assume values of 37.00 μm, 11.70 μm and 1.32 μm, respectively. An X-ray fluorescence analysis (XRF, Rigaku Supermini 2000, Tokyo, Japan) was conducted to evaluate the elemental composition in terms of oxides (Table 1).
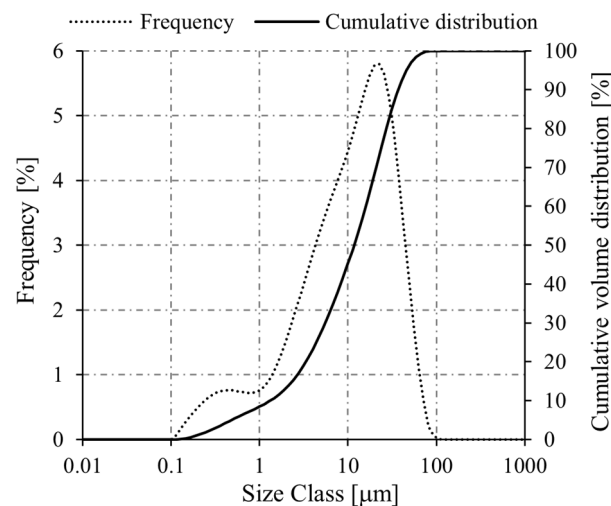
Figure 1. Particle size distribution of the as-received cement powder.

**Table 1.** XRF chemical composition of cement raw powder (wt.%).

CaO	SiO$_2$	SO$_3$	Al$_2$O$_3$	Fe$_2$O$_3$	MgO	K$_2$O	Na$_2$O	TiO$_2$	P$_2$O$_5$	SrO	MnO	LOI
64.5	17.9	4.3	4.2	3.5	1.3	0.9	0.4	0.4	0.1	0.1	0.1	2.1

The theoretical CO_2 uptake potential was evaluated based on the XRF chemical composition through the application of the modified Steinour equation [22], with an assumed value of 48.5%.

The chemical composition of the material was investigated by means of thermogravimetric differential thermal analysis (TG-DTA, LabSys evo machine, Setaram, Caluire-et-Cuire, France), carried out up to 1050 °C with a heating rate of 10 °C/min, with N_2 as carrier gas and on samples with a mass of 50 mg. X-ray diffraction analysis (XRD, Malvern Panalytical Empyrean, Worcestershire, United Kingdom) was carried out in a Bragg–Brentano configuration. The Cu-Kα wavelength radiation (0.15406 nm) was operated at 40 kV and 40 mA, with the 2θ spanning from 5° to 70° and an angular step of 0.006° held for 23 s. The diffractometer was equipped with Soller slits (0.04 rad), an anti-scatter slit (P7.5), a beam mask (10 mm), a divergence slit (¼°) and an axial slit (½°). XRD analysis was conducted to identify the crystalline phases present. Field emission Scanning Electron Microscopy (FE-SEM, Supra 40 Zeiss Merlin, Oberkochen, Germany) was employed to analyse the microstructure of the materials after the carbonation.

2.2. Aqueous CO_2 Mineralisation

The aqueous carbonation was conducted by stirring a suspension comprising cement powder while injecting CO_2 as a gas (Figure 2). The suspension, with a liquid-to-solid ratio of 3, comprised 240 g of demineralised water and 80 g of cement. The carbonation process was conducted under room pressure and temperature conditions, with a stirring rate of 1500 rpm. The CO_2 gas was provided by a cylinder with a flow of 200 L/h, with a purity of 99.9%. The high flow rate is essential to ensure the adequate dissolution of CO_2 in the suspension under open laboratory conditions, which allows for the significant release of the injected gas into the atmosphere. Potential industrial applications of the mineralisation process may include the recirculation of gas to prevent dispersion in the atmosphere and facilitate the utilisation of reduced CO_2 concentrations and/or flow rates.
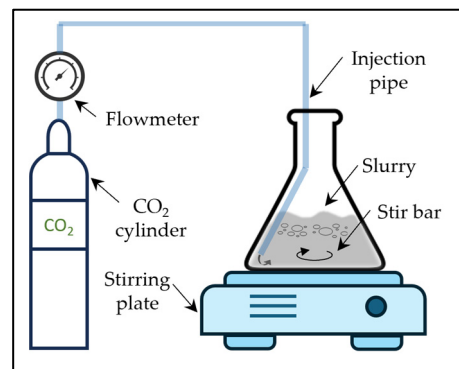
Figure 2. Setup of aqueous mineral carbonation process.

The duration of the carbonation process was varied, with experiments conducted for 5 min, 10 min, 20 min, 30 min and 40 min. Once the mineralisation process was complete, the carbonated cement powder was separated from the supernatant by means of centrifugation, followed by drying at 60 °C for 24 h. The efficiency of the mineralisation process was then assessed by quantifying the $CO_{2,uptake}$ of the processed powder. Two methods were employed to quantify the CO_2 content within the material: thermogravimetric analysis and thermal decomposition in a muffle furnace [23]. In accordance with the findings of several studies in this field [33–35], the release of CO_2 due to the decomposition of calcium carbonate decomposition is assumed to occur between 550 °C and 850 °C. The percentage of CO_2 content is calculated as the mass loss related to this temperature range, expressed as a percentage of the mass at 25 °C.

In the case of the thermogravimetric method, the mass values are obtained from the curves of the TG-DTA analysis. One sample, with an initial mass of 50 mg, was analysed for each carbonation test. The thermal decomposition in the muffle furnace consisted of a two-stage process: first, the sample was heated to 550 °C, and the weight was recorded; then, it was heated to 850 °C, and the weight was recorded. The percentage of CO_2 content was calculated as the difference between the two recorded weights, expressed as a percentage of the initial weight at 25 °C.

The initial mass of the samples subjected to thermal decomposition in a muffle furnace was approximately 2.5 g. Three replicates were conducted for each carbonation test, and the percentage of CO_2 content was assumed to be the average of the three values. The percentage of $CO_{2,uptake}$ was assessed using Equation (1):

$$\%CO_{2,uptake} = \frac{\%CO_{2,content} - \%CO_{2,initial}}{1 - \%CO_{2,content}} \qquad (1)$$

XRD analysis was conducted on samples of the processed powders to examine the alteration in the mineral composition of the cement under investigation over the course of the mineralisation process and to identify the compounds involved in the carbonation reactions.

3. Results and Discussion

3.1. Mineral Composition

Figure 3 presents the XRD patterns of the powders subjected to varying carbonation times. For comparison, the XRD pattern of the raw cement powder (Cem as-received) is also included as a reference.
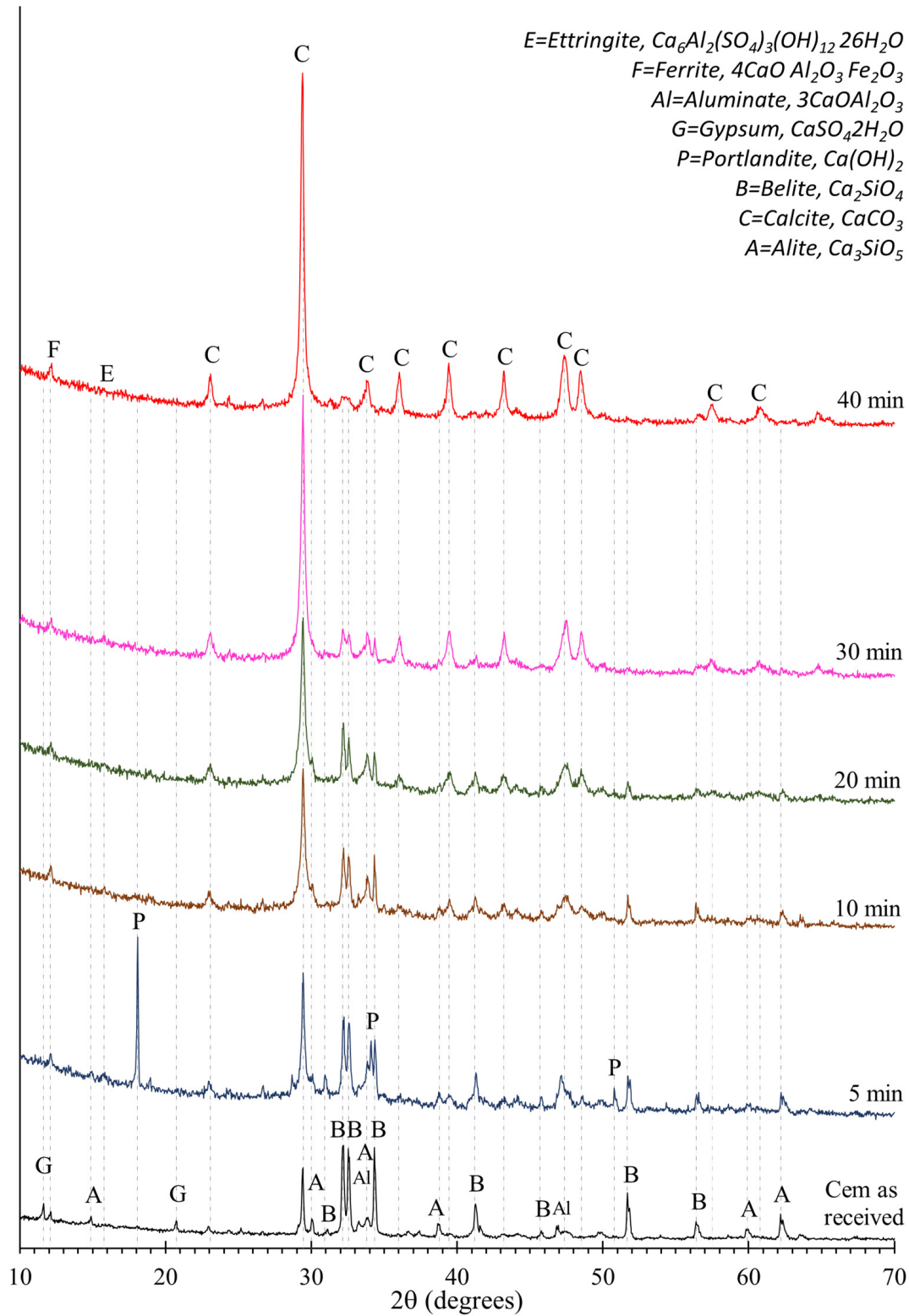
Figure 3. XRD pattern of as-received cement powder and powders at different times of carbonation.

The principal compounds identified in the raw material were calcium silicates, namely belite (C_2S) and alite (C_3S), calcium aluminates (C_3A), calcium ferroaluminates (C_4AF), and calcium sulphate (gypsum). Additionally, the presence of calcium carbonate was indicated by the identification of calcite peaks. At 5 min, the presence of portlandite is clearly identified, as evidenced by peaks at 2θ equal to 18.1° and 63.4°. The presence of $Ca(OH)_2$ is attributable to the commencement of the hydration process of calcium silicates, which results in the formation of calcium hydroxide.

Furthermore, the principal calcium carbonate peak, in the crystalline form of calcite, at 2θ equal to 29.4° is also markedly enhanced in comparison to the raw cement. This indicates that the carbonation process commences prior to the five minute mark. This finding is consistent with the literature, which indicates that the carbonation reaction of clinker in aqueous conditions occurs rapidly, with a reaction degree of alite phases equal to 15% after 0.5 min of carbonation [21]. However, the gypsum phase was not identified, while a slight signal attributed to the ettringite phase was observed. This is in line with expectations based on the reaction between calcium aluminates and calcium sulphate, which leads to ettringite formation.

The presence of other compounds already observed in the raw materials, alite and belite, can be still observed, indicating that the hydration process is not yet complete. Following a 10 min carbonation period, the portlandite peaks are no longer discernible, while the calcite peaks exhibit a notable intensification. It is also noteworthy that the alite signals exhibit a notable decline in intensity from the 10 min mark onward. Additionally, a reduction in the intensity of the belite phase can be observed as well, with a more pronounced decrease in the patterns starting from 30 min. These observations are consistent with the existing literature on the carbonation of cement, which associates this process with the formation of portlandite derived from the hydration of calcium silicates [36]. C_3S exhibits a rapid reaction, with a degree of reaction of approximately 80% after 10 min. C_2S, which commences the reaction process after 5 min, reaches a reaction degree of approximately 70% at 20 min [21].

Indeed, during the initial stages of the process, the dissolution of alite and precipitation of calcium carbonate result in a considerable consumption of CO_2, which is rapidly consumed at a rate that exceeds its solubility in the gas phase. Consequently, during this phase, the dissolution of CO_2 represents the limiting factor influencing the precipitation of calcium carbonate [21]. This explains the persistence of portlandite up to 5 min. Conversely, at longer carbonation times, the overall carbonation process is constrained by the dissolution of calcium silicates, as evidenced by the reduction of the intensity of their signal in the XRD spectrum and by the disappearance of portlandite.

Figure 4 illustrates the TG and DTA curves of the raw and mineralised cement at each specified carbonation time point. Regarding the raw powder, three main principal peaks in the DTA curve, corresponding to mass losses in the TG curve, were identified.

Peak I, occurring at approximately 140 °C, is associated with the dehydration of gypsum. Peak II, occurring at approximately 450 °C, is related to the dehydration of portlandite. Peak III, occurring at approximately 750 °C, is related to the decomposition of calcium carbonate. The mass loss associated with peak II is not substantial, indicating a relatively minor presence of portlandite. This conclusion is supported by the absence of a clear signal in the XRD pattern of the raw cement. The mass loss related to peak III, which is equal to 1.6%, represents the initial percentage of CO_2 content present in the raw material, $\%CO_{2,\text{initial}}$.

In accordance with the findings of the XRD analysis, the presence of portlandite (peak II) was identified at the 5 min carbonation stage, with a mass loss of 0.9% assessed via the tangent method [37]. Peak II is still discernible in the DTA curve at 10 min; however, no corresponding mass loss is evident in the TG curve, indicating a negligible amount of portlandite. No signals indicative of the presence of portlandite could be discerned at longer periods of carbonation.
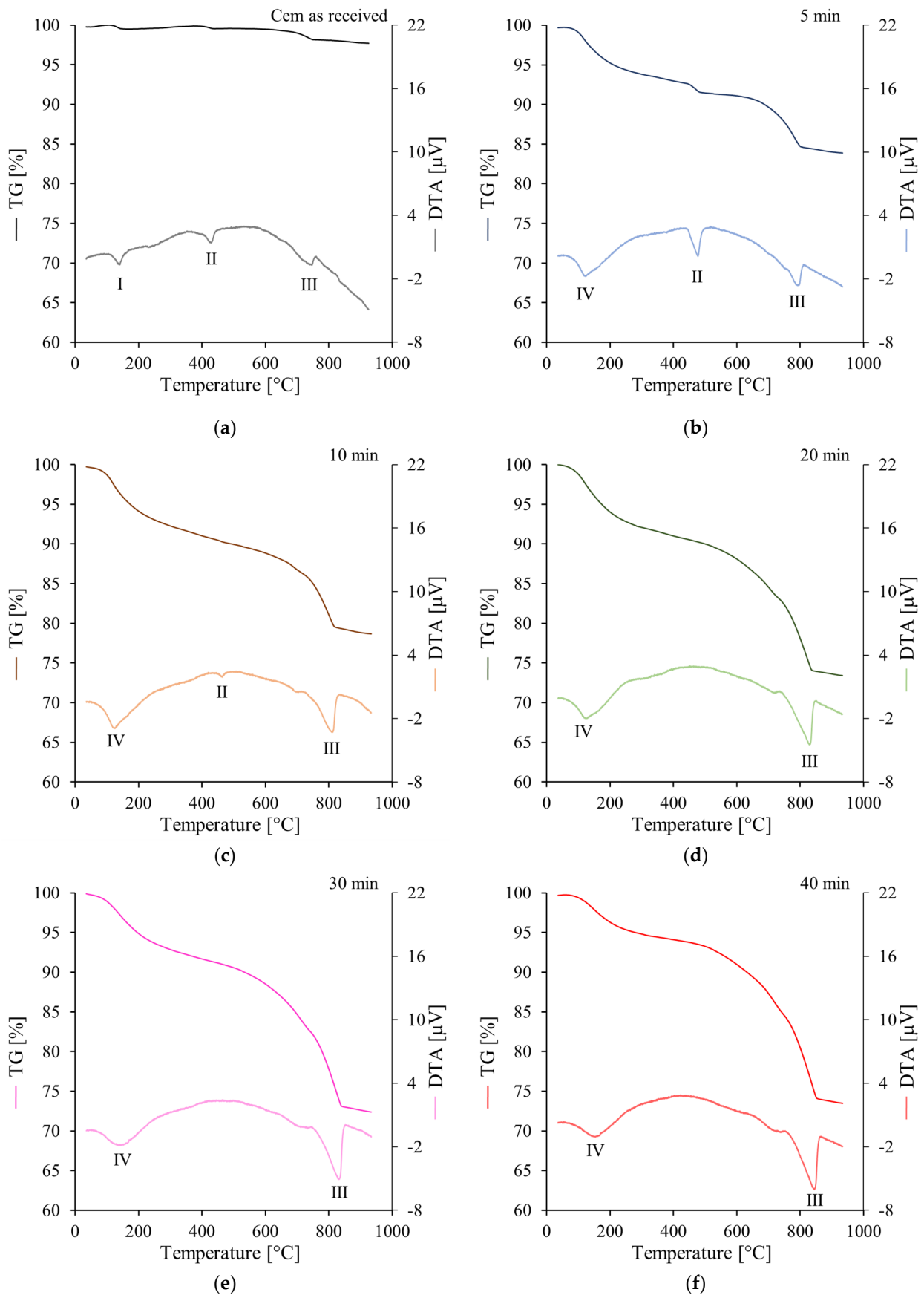
Figure 4. TG and DTA curves of (**a**) as-received cement powder and powders at times of carbonation of (**b**) 5 min; (**c**) 10 min; (**d**) 20 min; (**e**) 30 min; (**f**) 40 min.

The DTA curves of the carbonated samples display a peak between approximately 100 °C and 200 °C, which is indicative of the release of physically bonded water from the C-S-H gel. This confirms the occurrence of the silicate hydration process. The mass loss associated with peak III, resulting from the decomposition of calcium carbonate, is observed to increase with the process duration, indicating a higher degree of carbonation.

The analysis of mineral composition emphasises that in aqueous conditions, the process of hydration and carbonation occur concurrently, with carbonates formed through the conversion of portlandite derived from hydration. The presence of portlandite at a carbonation time of 5 min indicates that the dissolution of calcium silicate and the precipitation of calcite processes commence with a kinetic rate exceeding that of CO_2 dissolution, which does not permit the complete conversion of portlandite. At the 10 min mark, the absence of portlandite and the near total depletion of alite (as shown by a reduction in peak intensity), which reacts at a considerably faster rate than belite, may indicate that the limiting factor is the dissolution of silicates. Figure 5 depicts FE-SEM images of samples that have been carbonated for either 5 min or 40 min.
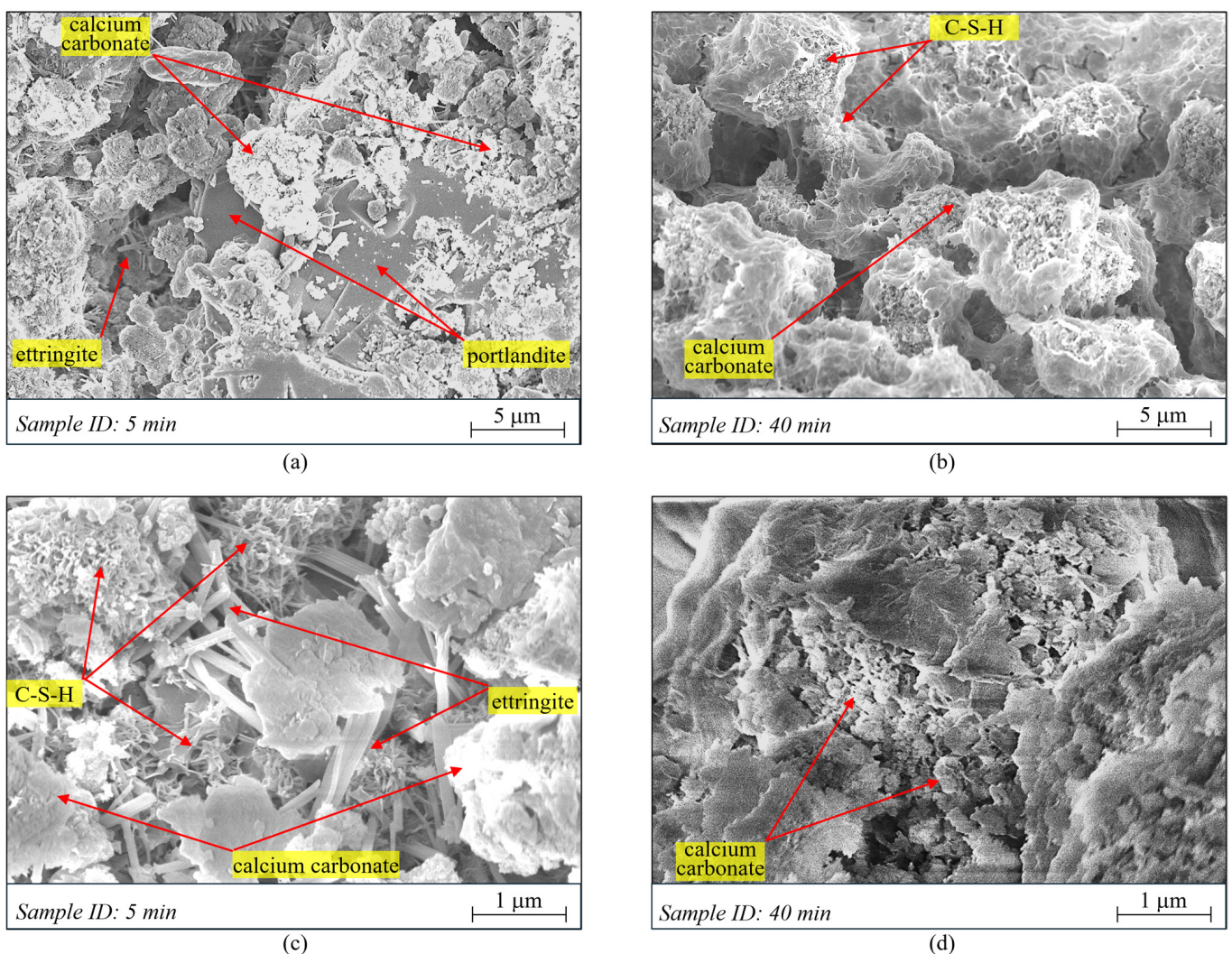
Figure 5. FE-SEM images of carbonated samples at (**a**) 5 min (Mag. 10,000×); (**b**) 40 min (Mag. 10,000×); (**c**) 5 min (Mag. 50,000×); (**d**) 40 min (Mag. 50,000×).

At 10,000× magnification, the sample carbonated for 5 min displays plate-like structures with hexagonal geometry, indicative of portlandite (Figure 5a). The elongated crystals, which are also discernible at 50,000× magnification (Figure 5c), indicate the presence of ettringite. Additionally, denser structures comprising grains that cover the portlandite

crystals and needle-like structures can be observed. While the images do not permit precise identification of these formations, their structures may be associated with the presence of calcium carbonate (presumably calcite) and C-S-H gel [38]. This finding is corroborated by the results of the XRD and TG-DTA analyses. Furthermore, the presence of a needle-like structure indicative of hydrated calcium silicates at an early age is consistent with the characteristics of C-S-H gel.

Similarly, images of samples subjected to 40 min treatment demonstrate the presence of needle-like formations, which can be attributed to the presence of C-S-H gel (Figure 5b). Moreover, the presence of regular grains forming compact structures that extensively cover the surface of the sample and that may be associated with the presence of calcium carbonate (Figure 5d). The presence of portlandite is detected in the 40 min sample. The compounds identified via FE-SEM analysis align with the results from XRD and TG-DTA, indicating the presence of calcium hydroxide that has not yet undergone carbonation at the 5 min mark and a higher presence of calcium carbonate at the 40 min mark, where any portlandite is observed.
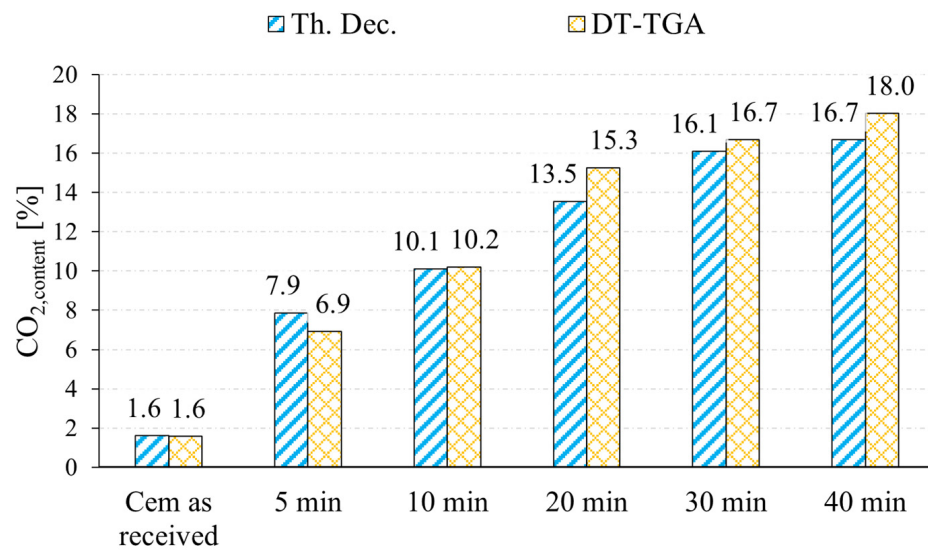
3.2. CO_2 Uptake

Three samples were subjected to thermal decomposition in a muffle furnace for each carbonation time. The CO_2 content, assessed by those decompositions for each test, along with the standard deviation, is presented in Table 2. The mean values derived from thermal decomposition in the muffle furnace, together with the values obtained from TG-DTA, are illustrated in Figure 6.

Table 2. $CO_{2,content}$ percentage (%) from Thermal Decomposition in a muffle furnace of as-received cement and carbonated samples; three replicates (I, II and III) and Standard Deviation (St. Dev.) for each carbonation test.

	$CO_{2,content}$ [%]			St. Dev. [%]
	I	II	III	
Cem as-received	1.6	1.6	1.6	0.01
5 min	7.8	7.9	7.9	0.04
10 min	10.2	10.1	10.1	0.04
20 min	13.5	13.6	13.6	0.08
30 min	16.0	16.1	16.2	0.08
40 min	16.8	16.6	16.6	0.14

Table 2 demonstrates that comparable outcomes are achieved with the two distinct methods. In greater detail, the measurements obtained via TG-DTA were found to be slightly higher than those obtained via thermal decomposition for times of carbonation exceeding 10 min. One possible explanation for this discrepancy is the difference in sample size between the two methods. The TG-DTA method was employed on a sample of approximately 50 mg, whereas the thermal decomposition method utilised samples of greater size, including three replicates of approximately 2.5 g each, which is more representative of the material. Alternatively, the lower value may be attributed to inadequate temperature control of the muffle furnace, with an actual temperature exceeding the set value of 550 °C, leading to an underestimation of CO_2 content.

Conversely, at a carbonation time of 5 min, the CO_2 content assessed via thermal decomposition in a muffle furnace was found to be higher than that estimated by TG-DTA. This discrepancy may be attributed to the operational parameters of the thermal decomposition method and the potential presence of portlandite. Following the initial heating phase at 550 °C, the sample is cooled, and the weight is recorded. It is then heated again up to 850 °C. During the interval between the two steps, portlandite may undergo partial carbonation due to the presence of CO_2 in the atmosphere, resulting in an overestimation.

Figure 6. CO_2 content of as-received cement and carbonated samples; average values from Thermal Decomposition in a muffle furnace (Th. Dec.) and estimates from the Thermogravimetric analysis (DT-TGA).

Table 3 presents the percentage of $CO_{2,uptake}$ values assessed by means of Equation (1), considering the average values derived from thermal decomposition measurements and the values from TG-DTA.

Table 3. $CO_{2,uptake}$ percentage (%) from thermal decomposition in a muffle furnace (average of the three replicates) and from TG-DTA of carbonated samples.

|	Th. Dec.	TG-DTA
	$CO_{2,uptake}$ [%]	$CO_{2,uptake}$ [%]
5 min	6.8	5.7
10 min	9.5	9.6
20 min	13.8	16.1
30 min	17.3	18.1
40 min	18.1	20.1

The results presented in Table 3 are illustrated in Figure 7, which depicts the equation describing the CO_2 uptake as a function of time during carbonation. The chart displays the curve that approximates the experimental data with a standard error of the estimate, S, equal to 0.37 %. Additionally, the equation of the trend line is provided for reference.

As anticipated, the CO_2 uptake increases with the duration of carbonation. In greater detail, the slope of the curve decreases with time and tends toward an asymptotic behaviour, indicating that the kinetics of the carbonation process slow down over time. Indeed, during the initial minutes of the process, the rate is limited by the dissolution of the CO_2 in water. However, after approximately 10 min, the dissolution of calcium silicates becomes the limiting factor. The progressive conversion of the compounds to be carbonated results in a reduction in their availability within the suspension, which in turn gives rise to the observed asymptotic trend.

In accordance with the projected trajectory, the CO_2 uptake observed at the 40 min mark is estimated to be approximately 70 % of the maximum attainable value (asymptote). The high degree of carbonation observed after 40 min is in accordance with the findings of previous studies investigating the evolution of pH during carbonation. Initially, a notable increase in pH is caused by the dissolution of calcium silicates. However, after approximately ten min, there is a significant decline in pH as the degree of carbonation increases, reaching a nearly constant value after about 40 min [21]. Nevertheless, additional

experimental tests at extended durations are necessary to substantiate the hypothesis, as other variables may influence the carbonation process.
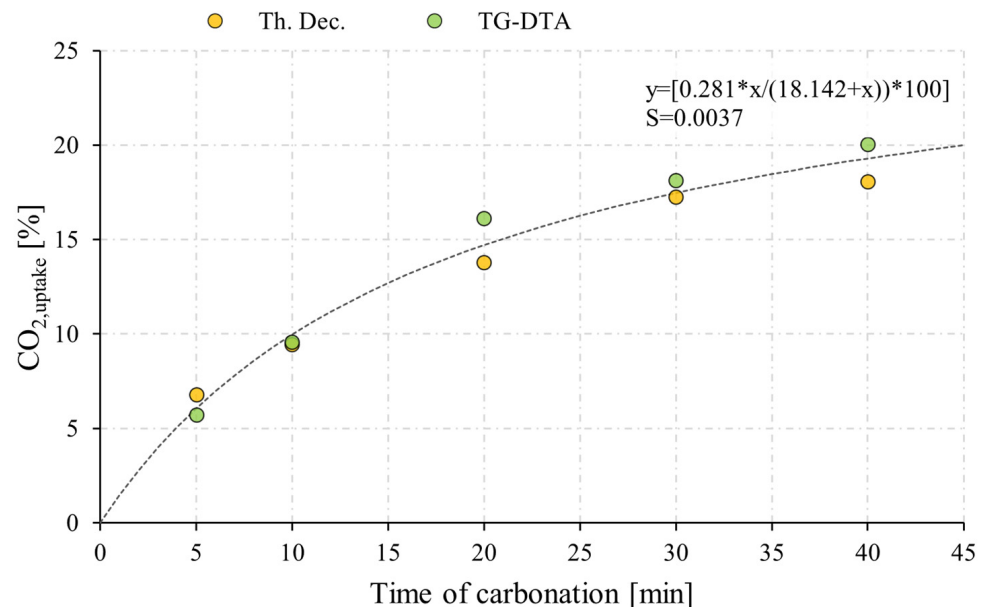
Figure 7. CO_2 uptake versus time of carbonation; values from Th. Dec. and TG-DTA; trendline with equation and standard error of the estimate (S).

According to the theoretical CO_2 uptake evaluated via the Steinour equation, the carbonation efficiency (ratio between experimental and theoretical values) reaches a value of 39.3% at 40 min.

4. Comparison with Other Cement-Based Materials Carbonated in Aqueous Conditions

The present study compared the carbonation efficiency of cement powder subjected to aqueous mineralisation with the findings of previous research investigating the accelerated carbonation of cementitious powders via the same process. The objective of the comparison is twofold: firstly, to verify that the results align with those of similar studies, and secondly, to identify the potential strategies for improving the efficiency of the process.

The comparison studies either involve cement powder as the raw material [20] or pulverised hydrated cementitious paste created in the laboratory [26,29,30] or from construction and demolition waste [27,28].

Table 4 presents a summary of the material types, operational parameters (liquid-to-solid ratio, CO_2 concentration and flow, pressure, temperature and time of carbonation), and the CO_2 uptake for all the considered studies. It should be noted that studies reporting pressure values higher than those in ambient conditions adopted closed systems in which the carbonation process occurred in an autoclave apparatus.

In a series of experiments conducted by Fu et al. (2024), cement powder was carbonated under similar operational conditions to those employed in the present study, including liquid-to-solid ratio, pressure and temperature. Additionally, the influence of carbonation time was investigated, extending up to 40 min [20]. Similarly, as in the present study, an increase in the degree of carbonation with time was observed. Nevertheless, the attained CO_2 uptake values were markedly lower. This may be attributed to the low CO_2 flow rate employed, which was one order of magnitude lower than that used in this study and represented a potential limiting factor of the process. A comparison of the rate at which the carbonation degree increases over time reveals that doubling the process duration from 10 to 20 min in both studies results in a CO_2 uptake approximately 1.5 times higher while increasing the time from 10 to 40 min in both studies leads to a CO_2 uptake that is approximately twice as high. This demonstrates that in both systems, the carbonation degree increased with time at comparable rates, irrespective of the disparate CO_2 flow conditions.

Teune et al. (2023) employed ambient operational conditions in a manner consistent with the present study, yet they permitted significantly longer periods of carbonation [26]. This may be attributed to the lower CO_2 flow and concentration employed. It is noteworthy that the two CO_2 uptake values, 20% and 32%, are associated with pastes produced, respectively, with cement of type CEM-III 42.5 N (70% blast furnace slag) and CEM-I 52.5 R (OPC). This result serves to highlight the enhanced reactivity of OPC in comparison to alternative types. The CO_2 uptake value attained by the CEM-I-related powder is comparable to the maximum value predicted by the trend line in Figure 7 (~28%), thereby confirming that the complete carbonation may occur at a high process duration.

Table 4. Comparison with other cement-based materials subjected to carbonation processes.

	Study	Material	Liquid-to-Solid Ratio	CO_2 Conc.	CO_2 Flow	Pressure	Temperature	Time	CO_2 Uptake
	This study	cement powder	3	100%	200 L/h	ambient	ambient	5 m 10 m 20 m 30 m 40 m	6.3% 9.5% 15.0% 17.7% 19.1%
[20]	Fu et al., 2024	cement powder	2	100%	12 L/h	ambient	ambient	10 m 20 m 40 m	3.6% 5.3% 8.2%
[26]	Teune et al., 2023	hydrated cement paste	10	15%	10 L/h	ambient	ambient	5 h ÷ 6 h	20% ÷ 32%
[27]	Ho et al., 2021	cement concrete waste	100	14%	240 L/h	-	ambient	1.5 h	4% ÷ 13%
[28]	Pasquier et al., 2018	cement concrete waste	10	18%	-	10.2 bar	ambient	15 min	7% ÷ 11%
[29]	Kong et al., 2022	hydrated cement paste *	2.5	100%	-	10 bar 20 bar 25 bar	60 °C	24 h	20.7% 20.8% 24.3%
[30]	** Hernandez-Rodriguez et al., 2021	hydrated cement paste	15	100%	-	11 bar	ambient	1 h 3 h 6 h 21 h 67 h 97 h 120 h	14% 22% 24% 23% 29% 21% 30%
		hydrated cement paste	15	100%	-	1 bar 11 bar 31 bar 51 bar	ambient	6 h	29% 28% 29% 28%

* hydrated and aged cement paste simulating cement paste from demolished concrete. ** CO_2 uptake was calculated by means of Equation (1) based on the CO_2 content data available in the article.

Ho et al. (2021) [27], who employed operational parameters analogous to those of the present study and a carbonation time with the same order of magnitude, demonstrated lower CO_2 uptake values. This can be attributed to the reduced reactivity of the waste concrete in comparison to the raw cement, as well as the higher initial CO_2 content present in the material. The results presented by Pasquier et al. (2018) [28] demonstrate that a comparable degree of carbonation can be achieved in a considerably shorter time frame and with significantly higher pressure. Significantly higher CO_2 uptake values were observed by Kong et al. (2022) [29], in which the carbonation was conducted at high pressure and temperature conditions, with a particular process including pretreatment of the powder via calcination.

Hernandez-Rodriguez et al. (2021) conducted an analysis to determine the influence of both pressure and time of carbonation [30]. Their study demonstrates that at the shorter time interval of 1 h, a CO_2 uptake value of approximately 14% is observed. In contrast, for all tests conducted over longer periods of time, the CO_2 uptake exhibits a notable increase, ranging from 21% to 30%. Additionally, it is noteworthy that when a prolonged

carbonation time of 6 h is employed, the carbonation degree remains unaltered, irrespective of the high-pressure conditions.

The comparison with the literature shows that numerous studies utilising hydrated pastes have employed significantly longer periods of carbonation. Indeed, the carbonation of raw OPC powder (i.e., not pre-hydrated) is characterised by a higher rate and attains a similar carbonation degree in shorter times. This is a significant factor to be taken into account in the case of the utilisation of waste cement paste that has already undergone a prior hydration process. The data also demonstrate that high carbonation degrees are achieved when high temperature and pressure values are employed [29,30], thereby confirming the significance of these operational parameters in enhancing the efficiency of the aqueous carbonation process. In light of these findings, further investigation is required to quantify the beneficial effects associated with the increase in temperature and pressure while also considering the carbon footprint associated with the use of more severe operational parameters.

In conclusion, the comparison with the literature demonstrates that carbonation in aqueous conditions and the use of OPC powder results in CO_2 uptake values comparable to those of other studies despite the use of ambient temperature and pressure conditions. This is a pivotal consideration in the context of a cost-benefit analysis of potential applications where these processes could be deployed. The aqueous carbonation of cement powder can be employed to facilitate the formation of carbonates in fresh mixtures. In this regard, the utilisation of mild operational conditions (ambient temperature and pressure and relatively brief periods of carbonation) represents a favourable aspect that may facilitate the potential applications. Furthermore, the comparison demonstrates that the utilisation of reduced CO_2 flows, despite the retardation of carbonation reactions, still yields an effective process. This aspect should be considered in view of potential applications in which industrial flue gas may be used as a CO_2 supplier. In this regard, further investigation is required to explore the feasibility of integrating the mineralisation process with the management of CO_2-rich gases emitted by industrial plants.

5. Conclusions

This study investigates the evolution of the carbonation degree over time during the aqueous mineralisation process utilising cement powder. We present an analysis of both the carbonation degree and the mineral composition. Our principal findings are presented as follows:

- The XRD pattern analysis indicates that the intensity of peaks associated with calcium silicates diminishes as a consequence of the hydration and carbonation processes. Conversely, a significant increase in the intensity of calcium carbonate peaks with the carbonation time is observed.
- From both the TG-DTA and XRD analysis, the presence of portlandite at a carbonation time of 5 min is observed, while it is not shown from 10 min upward. This may indicate that the rate of CO_2 dissolution from the gas is the limiting factor of the carbonation process during the initial minutes. Conversely, at longer durations of the process, with C_3S (alite) almost fully reacted, and with C_2S (belite) characterised by a slower reaction rate, silicate dissolution represents the limiting factor of the process.
- The thermal decomposition in a muffle furnace and TG-DTA emerge as valuable methods for the assessment of CO_2 content in carbonated materials, with comparable results. The TG-DTA results to be more appropriate when portlandite is present in the material.
- The CO_2 uptake increases with the time of carbonation, following a trend of asymptotic behaviour. The trendline prediction curve indicates that CO_2 uptake, with a value of 19.1%, reaches approximately 70% of the maximum achievable value at 40 min.
- The comparison with the literature emphasises the attainment of significant CO_2 uptake values despite the use of mild and less energy-demanding operational parameters. Furthermore, it highlights the enhanced carbonation capacity of raw OPC in

comparison to hydrated cement pastes, including those derived from construction and demolition waste materials.

This article offers a valuable contribution to the field by defining the carbonation degree evolution of cement powder subjected to aqueous mineralisation. It provides a crucial reference point for the definition of the operational parameters of treatments in which the calcium carbonate content must be controlled. In this regard, a suitable application is represented by processes combining carbonation with the mixing process to produce fresh concrete. It is noteworthy that this study was conducted using a suspension with a liquid-to-solid ratio equal to 3. Future research should consider varying ratios in line with specific applications under investigation.

The equation predicting the evolution of the CO_2 uptake over the time of carbonation can be employed in studies aimed at optimising the mineralisation technique by balancing the emissions associated with the length of the process with the stored CO_2 to achieve an optimal balance between the two.

Finally, our study paves the way for further analysis aimed at defining the applicability of the mineralisation process to the production of building materials. In particular, the impact of carbonation degrees on the strength development should be investigated, with a specific focus on the hydration and/or pozzolanic reactions, as well as the potential nucleation effects that may occur when the processed powders are used in conjunction with traditional binders.

References

1. Coppola, L.; Bellezze, T.; Belli, A.; Bianco, A.; Blasi, E.; Cappello, M.; Caputo, D.; Chougan, M.; Coffetti, D.; Coppola, B.; et al. New materials and technologies for durability and conservation of building heritage. *Materials* **2023**, *16*, 1190. [CrossRef]
2. Busch, P.; Kendall, A.; Murphy, C.W.; Miller, S.A. Literature review on policies to mitigate GHG emissions for cement and concrete. *Resour. Conserv. Recycl.* **2022**, *182*, 106278. [CrossRef]
3. CEMBUREAU. The European Cement Association 2021. In *Cementing the European Green Deal: Reaching Climate Neutrality Along the Cement and Concrete Value Chain by 2050*; CEMBUREAU: Brussels, Belgium, 2021.
4. Ferrara, G.; Martinelli, E. Tensile behaviour of Textile Reinforced Mortar composite systems with flax fibres. In Proceedings of the 12th Fib International PhD Symposium in Civil Engineering 2018, Prague, Czech Republic, 29–31 August 2018; pp. 863–869.
5. Pepe, M.; Lombardi, R.; Ferrara, G.; Agnetti, S.; Martinelli, E. Experimental Characterisation of Lime-Based Textile-Reinforced Mortar Systems Made of Either Jute or Flax Fabrics. *Materials* **2023**, *16*, 709. [CrossRef]
6. Reboul, N.; Saidi, M.; Mualla, S.; Homoro, O.; Amziane, S. Bond behaviour of Fibre Reinforced Polymers applied on masonry substrate: Analysis based on acoustic emission, digital image correlation and analytical modelling. *Constr. Build. Mater.* **2023**, *403*, 132921. [CrossRef]
7. Ferrara, G.; Michel, L.; Ferrier, E. Flexural behaviour of timber-concrete composite floor systems linearly supported at two edges. *Eng. Struct.* **2023**, *281*, 115782. [CrossRef]
8. Bolden, J.; Abu-Lebdeh, T.; Fini, E. Utilization of recycled and waste materials in various construction applications. *Am. J. Env. Sci.* **2013**, *9*, 14–24. [CrossRef]

9. Pan, S.Y.; Chang, E.E.; Chiang, P.C. CO_2 capture by accelerated carbonation of alkaline wastes: A review on its principles and applications. *AAQR* **2012**, *12*, 770–791. [CrossRef]
10. Ferrara, G.; Belli, A.; Keulen, A.; Razo, D.A.S.; Tulliani, J.; Palmero, P. Carbon sequestration in Steel Slag-based mortar: Investigation on chemical composition and mechanical properties. In Proceedings of the 2nd Fib Italy YMG Symposium on Concrete and Concrete Structures 2021, Rome, Italy, 18–19 November 2021; pp. 220–227.
11. Mahoutian, M.; Shao, Y. Production of cement-free construction blocks from industry wastes. *J. Clean. Prod.* **2016**, *137*, 1339–1346. [CrossRef]
12. Bonfante, F.; Ferrara, G.; Humbert, P.; Garufi, D.; Tulliani, J.M.C.; Palmero, P. CO_2 Sequestration Through Aqueous Carbonation of Electric Arc Furnace Slag. *JACT* **2024**, *22*, 207–218. [CrossRef]
13. Polettini, A.; Pomi, R.; Stramazzo, A. CO_2 sequestration through aqueous accelerated carbonation of BOF slag: A factorial study of parameters effects. *J. Environ. Manag.* **2016**, *167*, 185–195. [CrossRef]
14. Bonfante, F.; Humbert, P.; Tulliani, J.M.; Palmero, P.; Ferrara, G. CO_2 uptake of cement by-pass dust via direct aqueous carbonation: An experimental design for time and temperature optimisation. *Mater. Struct.* **2024**, *57*, 181. [CrossRef]
15. Ma, M.; Mehdizadeh, H.; Guo, M.Z.; Ling, T.C. Effect of direct carbonation routes of basic oxygen furnace slag (BOFS) on strength and hydration of blended cement paste. *Constr. Build. Mater.* **2021**, *304*, 124628. [CrossRef]
16. Fang, Y.; Su, W.; Zhang, Y.; Zhang, M.; Ding, X.; Wang, Q. Effect of accelerated precarbonation on hydration activity and volume stability of steel slag as a supplementary cementitious material. *J. Therm. Anal. Calorim.* **2022**, *147*, 6181–6191. [CrossRef]
17. Lippiatt, N.; Ling, T.C.; Eggermont, S. Combining hydration and carbonation of cement using super-saturated aqueous CO_2 solution. *Constr. Build. Mater.* **2019**, *229*, 116825. [CrossRef]
18. Monkman, S.; MacDonald, M.; Hooton, R.D.; Sandberg, P. Properties and durability of concrete produced using CO_2 as an accelerating admixture. *Cem. Concr. Compos.* **2016**, *74*, 218–224. [CrossRef]
19. Matschei, T.; Lothenbach, B.; Glasser, F.P. The role of calcium carbonate in cement hydration. *Cem. Concr. Res.* **2007**, *37*, 551–558. [CrossRef]
20. Fu, X.; Guerini, A.; Zampini, D.; Rotta Loria, A.F. Storing CO_2 while strengthening concrete by carbonating its cement in suspension. *Commun. Mater.* **2024**, *5*, 109. [CrossRef]
21. Zajac, M.; Lechevallier, A.; Durdzinski, P.; Bullerjahn, F.; Skibsted, J.; Haha, M.B. CO_2 mineralisation of Portland cement: Towards understanding the mechanisms of enforced carbonation. *J. CO_2 Util.* **2020**, *38*, 398–415. [CrossRef]
22. Huntzinger, D.N.; Gierke, J.S.; Kawatra, S.K.; Eisele, T.C.; Sutter, L.L. Carbon dioxide sequestration in cement kiln dust through mineral carbonation. *Environ. Sci. Technol.* **2009**, *43*, 1986–1992. [CrossRef]
23. Ferrara, G.; Belli, A.; Keulen, A.; Tulliani, J.M.; Palmero, P. Testing procedures for CO_2 uptake assessment of accelerated carbonation products: Experimental application on basic oxygen furnace steel slag samples. *Constr. Build. Mater.* **2023**, *406*, 133384. [CrossRef]
24. Librandi, P.; Nielsen, P.; Costa, G.; Snellings, R.; Quaghebeur, M.; Baciocchi, R. Mechanical and environmental properties of carbonated steel slag compacts as a function of mineralogy and CO_2 uptake. *J. CO_2 Util.* **2019**, *33*, 201–214. [CrossRef]
25. RILEM Technical Committee 309-MCP: Accelerated Mineral Carbonation for the Production of Construction Materials 2022. Chair: Snellings, R. Available online: https://www.rilem.net/groupe/309-mcp-accelerated-mineral-carbonation-for-the-production-of-construction-materials-442 (accessed on 27 October 2024).
26. Teune, I.E.; Schollbach, K.; Florea, M.V.A.; Brouwers, H.J.H. Carbonation of hydrated cement: The impact of carbonation conditions on CO_2 sequestration, phase formation, and reactivity. *J. Build. Eng.* **2023**, *79*, 107785. [CrossRef]
27. Ho, H.J.; Iizuka, A.; Shibata, E.; Tomita, H.; Takano, K.; Endo, T. Utilization of CO_2 in direct aqueous carbonation of concrete fines generated from aggregate recycling: Influences of the solid-liquid ratio and CO_2 concentration. *J. Clean. Prod.* **2021**, *312*, 127832. [CrossRef]
28. Pasquier, L.C.; Kemache, N.; Mocellin, J.; Blais, J.F.; Mercier, G. Waste concrete valorization; aggregates and mineral carbonation feedstock production. *Geosciences* **2018**, *8*, 342. [CrossRef]
29. Kong, Y.; Song, Y.; Weng, Y.; Kurumisawa, K.; Yan, D.; Zhou, X.; Wang, S.; Ruan, S. Influences of CO_2-cured cement powders on hydration of cement paste. *Greenh. Gases* **2022**, *12*, 249–262. [CrossRef]
30. Hernandez-Rodriguez, A.; Orlando, A.; Montegrossi, G.; Huet, B.; Virgili, G.; Vaselli, O. Experimental analysis on the carbonation rate of Portland cement at room temperature and CO_2 partial pressure from 1 to 51 bar. *Cem. Concr. Compos.* **2021**, *124*, 104271. [CrossRef]
31. Xi, F.; Davis, S.J.; Ciais, P.; Crawford-Brown, D.; Guan, D.; Pade, C.; Shi, T.; Syddall, M.; Lv, J.; Ji, L. Substantial global carbon uptake by cement carbonation. *Nat. Geosci.* **2016**, *9*, 880–883. [CrossRef]
32. Ashraf, W. Carbonation of cement-based materials: Challenges and opportunities. *Constr. Build. Mater.* **2016**, *120*, 558–570. [CrossRef]
33. Mo, L.; Zhang, F.; Deng, M. Mechanical performance and microstructure of the calcium carbonate binders produced by carbonating steel slag paste under CO_2 curing. *Cem. Concr. Res.* **2016**, *88*, 217–226. [CrossRef]
34. Moon, E.J.; Choi, Y.C. Development of carbon-capture binder using stainless steel argon oxygen decarburization slag activated by carbonation. *J. Clean. Prod.* **2018**, *180*, 642–654. [CrossRef]
35. Liu, G.; Schollbach, K.; van der Laan, S.; Tang, P.; Florea, M.V.; Brouwers, H.J.H. Recycling and utilization of high volume converter steel slag into CO_2 activated mortars–The role of slag particle size. *Resour. Conserv. Recycl.* **2020**, *160*, 104883. [CrossRef]

36. de Sena Costa, B.L.; de Oliveira Freitas, J.C.; Santos, P.H.S.; de Araújo Melo, D.M.; de Oliveira, Y.H. Effects of carbon dioxide in Portland cement: A relation between static sedimentation and carbonation. *Constr. Build. Mater.* **2017**, *150*, 450–458. [CrossRef]

37. Lothenbach, B.; Durdzinski, P.; De Weerdt, K. *Thermogravimetric Analysis. A Practical Guide to Microstructural Analysis of Cementitious Materials*; Crc Press: Boca Raton, FL, USA, 2016; Volume 1, pp. 177–211.

38. Zhang, D.; Wang, Y.; Ma, M.; Guo, X.; Zhao, S.; Zhang, S.; Yang, Q. Effect of equal volume replacement of fine aggregate with fly ash on carbonation resistance of concrete. *Materials* **2022**, *15*, 1550. [CrossRef]